Volume 1 | Number 1 | Jan 2013 | Pages 1–100

Catalysis Science & Technology

www.rsc.org/catalysis

ROYAL SOCIETY OF CHEMISTRY

www.rsc.org/catalysis
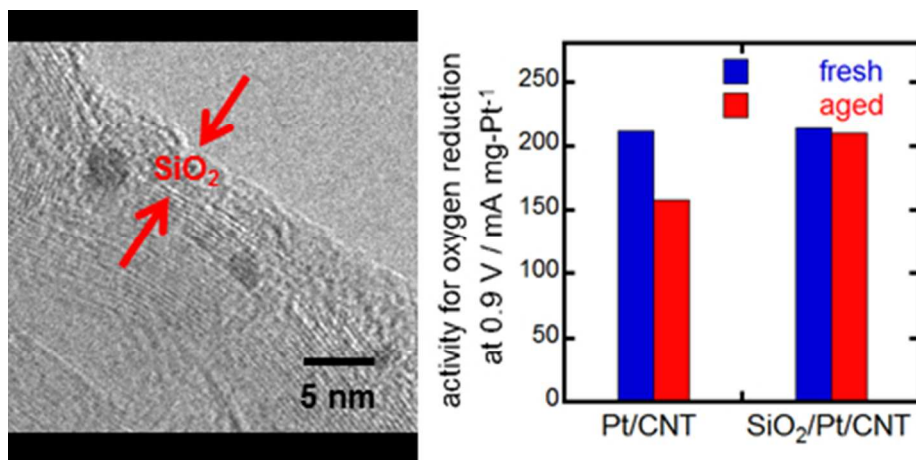
78x38mm (150 x 150 DPI)

Highly active and durable silica-coated Pt cathode catalysts for polymer electrolyte fuel cells: control of micropore structures in silica layers

Sakae Takenaka,[*a,b,c] Takahiro Miyazaki,[a] Hideki Matsune[a] and Masahiro Kishida[a]

[a] Department of Chemical Engineering, Graduate School of Engineering, Kyushu University, Moto-oka 744, Nishi-ku, Fukuoka 819-0395, Japan

[b] PRESTO, Japan Science and Technology Agency (JST), 4-1-8 Honcho Kawaguchi, Saitama 332-0012, Japan

[c] International Institute for Carbon Neutral Energy Research (I2CNER), Kyushu University, Moto-oka 744, Nishi-ku, Fukuoka 819-0395, Japan

E-mail: takenaka@chem-eng.kyushu-u.ac.jp

Author for correspondence:
Sakae Takenaka
Department of Chemical Engineering
Graduate School of Engineering
Kyushu University
Moto-oka 744, Nishi-ku, Fukuoka 819-0395, Japan
Tel & Fax: +81-92-802-2752
E-mail: takenaka@chem-eng.kyushu-u.ac.jp

1

Abstract

Carbon nanotube (CNT)-supported Pt catalysts (Pt/CNT) for use as cathode components

in polymer electrolyte fuel cells (PEFCs) were covered with silica layers to prevent

particle size increases during operation of the PEFC, either through sintering of the Pt

particles or the dissolution and redeposition of Pt ions. The formation of silica layers by

the successive hydrolysis of 3-aminopropyltriethoxysilane (APTES) and

tetraethoxysilane (TEOS) significantly improved the durability of the Pt/CNT catalysts

under cathodic conditions, although the activity of the silica-coated material for the

oxygen reduction reaction was slightly lower than that of the uncoated catalyst. In

contrast, a silica-coated Pt/CNT catalyst prepared by the successive hydrolysis of

APTES and TEOS in the presence of NH_2-$(CH_2)_n$-NH_2 (n = 6, 8 and 10) exhibited both

high catalytic activity and excellent durability. The NH_2-$(CH_2)_n$-NH_2 added during the

silica coating process worked as a template for the formation of micropores in the silica

layers and the resulting pore structures enhanced the diffusion of both reactants and

products during oxygen reduction on the silica-coated Pt/CNT catalysts.

2

1. Introduction

The reduction of Pt loading is one of most challenging issues preventing the widespread commercialization of polymer electrolyte fuel cells (PEFCs). In such devices, Pt metal is used as a catalytically active metal component for the oxygen reduction reaction (ORR) at the cathode and for the hydrogen oxidation reaction (HOR) at the anode. The Pt loading at the cathode is significantly higher than at the anode because of the sluggish kinetics of the ORR on Pt catalysts compared with that of the HOR. Ideally, then, it would be beneficial to lower the Pt loading at the cathode. In practice, however, this is very difficult, since the cathode catalysts are severely deactivated during operation of the PEFC.[1-4] The Pt cathode catalyst must also work under severe conditions, including low pH, high positive potential, an oxygen atmosphere and high temperatures. Pt metal particles can also readily migrate on carbon supports to grow larger particles under cathodic conditions. In addition, Pt metal particles can dissolve at the cathode to form Pt cations that deposit on existing Pt particles, resulting in additional particle growth. These increases in the sizes of Pt particles during PEFC operation should be avoided in order to reduce the Pt loading in PEFCs.

The growth of metal particles, especially that of precious metal particles during catalytic reactions, is a common subject in catalyst research. Supported precious metal

particles such as Pt, Rh and Pd have been utilized as catalysts for the purification of automobile exhaust gases, the cracking of hydrocarbons and naphtha, and the synthesis of fine chemicals. These particles are also easily aggregated during such reactions because these processes are typically performed under severe conditions, including high temperatures and pressures. Recently, core-shell catalysts have been developed to improve the sintering tolerance of precious metal particles.[5-9] In this process, supported metal particles or bare metal particles are covered with a layer of a metal oxide such as silica. The metal particles covered with silica layers are not in contact with one another and so the coverage improves the durability of the catalysts.

We have also covered carbon-supported Pt catalysts with silica layers[10,11] and these silica-coated Pt catalysts have been utilized as highly durable cathode catalysts for PEFCs.[12,13] Carbon-supported Pt catalysts are normally severely deactivated during the operation of a PEFC, but coverage of the Pt catalyst with a silica layer mitigates increases in the Pt particle sizes, since the silica layer prevents the migration of particles on carbon supports and also restricts the diffusion of dissolved Pt cations. These silica-coated Pt catalysts have thus exhibited high durability under PEFC cathode conditions. However, the coverage of Pt catalysts with silica layers also slightly decreased their activity for the ORR.[14] This occurred because oxygen molecules and

4

protons, the reactants in the ORR, must migrate through the silica layers to the Pt metal

surfaces, while water molecules as the product must diffuse from the metal surfaces

outward through the silica layers. The silica layers thus act as diffusion barriers for the

reactants and products. Silica layers on Pt catalysts have been prepared by the

successive hydrolysis of 3-aminopropyltriethoxysilane (APTES) and tetraethoxysilane

(TEOS) and it is likely that the pore sizes of the silica layers prepared from APTES and

TEOS are too small to allow ready diffusion of the reactants and products. However, the

porous structure of the silica in silica-coated catalysts has been frequently controlled.

For example, the hydrolysis and polycondensation of TEOS in the presence of

surfactants such as tetraalkylammonium chloride and triblock copolymers has been

shown to form mesoporous silica, since surfactant micelles work as templates for

mesopore formation.[15,16] The resulting mesopores in the silica layers, however, are too

large to prevent the diffusion of Pt cations out of the silica layers. In the present study,

we prepared silica-coated Pt catalysts by the successive hydrolysis of APTES and TEOS

in the presence of $NH_2-(CH_2)_n-NH_2$ (n = 6, 8 and 10). In the former processes,

surfactant molecules such as triblock copolymers underwent self-assembly to form

micelles during the preparation of mesoporous silica. In contrast, the $NH_2-(CH_2)_n-NH_2$

used in the present study did not form micelles, because the amount of $NH_2-(CH_2)_n-NH_2$

added was very small, but rather acted as molecular templates to promote the formation

of micropores in the silica. In the present paper, we demonstrate that silica-coated Pt

catalysts prepared by the successive hydrolysis of APTES and TEOS in the presence of

NH_2-$(CH_2)_n$-NH_2 exhibit both high durability and high activity for the ORR.

2. Experimental

2.1 Preparation of catalysts

Carbon-supported Pt catalysts were prepared using a conventional impregnation

method, and multi-walled carbon nanotubes (CNTs) were used as supports to avoid the

deactivation of the Pt catalysts by carbon corrosion.[17,18] CNTs are highly stable under

PEFC cathode conditions due to the high degree of graphitization of this material. The

CNTs were dispersed in an aqueous solution of $Pt(NO_3)_2(NH_3)_2$ at 333 K and the

solution was then dried. The dried samples were subsequently treated with hydrogen at

523 K to obtain CNT-supported Pt catalysts (Pt/CNT; Pt loading = 15 wt%).

Silica-coated Pt/CNT (SiO_2/Pt/CNT) materials were prepared by the successive

hydrolysis of APTES and TEOS.[19,20] In this process, the Pt/CNT (0.10 g) material was

ultrasonically dispersed in water (22 mL) and the pH of the solution was adjusted to

approximately 11 by the addition of aqueous NH_3. The resulting dispersion was stirred

6

at 333 K for 30 min after the addition of APTES (0.07 g). Subsequently TEOS (0.10 g) was added to the solution and the mixture was stirred for a further 90 min at 333 K. Finally, the samples were reduced with hydrogen at 623 K. SiO_2/Pt/CNT catalysts were also prepared by the successive hydrolysis of APTES and methyltriethoxysilane (MTEOS) using a method similar to that described above.[14] Silica layers prepared from MTEOS contained methyl groups since the CH_3-Si bonds in MTEOS were not hydrolyzed under our preparation conditions. Thus, the surface properties of silica layers prepared from MTEOS would have been more hydrophobic compared to that of silica prepared from TEOS. SiO_2/Pt/CNT catalysts prepared from APTES and TEOS or from APTES and MTEOS were denoted as SiO_2/Pt/CNT(TEOS) or SiO_2/Pt/CNT(MTEOS), respectively.

SiO_2/Pt/CNT was also prepared by the successive hydrolysis of APTES and TEOS in the presence of NH_2-$(CH_2)_n$-NH_2 (n = 6, 8 and 10). In this process, samples of the Pt/CNT catalyst (0.10 g) were ultrasonically dispersed in water (22 mL) and the pH of the suspension was adjusted to approximately 11 by the addition of aqueous NH_3. After addition of APTES (0.07 g), NH_2-$(CH_2)_n$-NH_2 (0.20 mmol) was added to the solution. TEOS (0.10 g) was subsequently added and then hydrolyzed for 90 min at 333 K, after which the samples were reduced with hydrogen at 623 K. The SiO_2/Pt/CNT catalysts

7

prepared in the presence of $NH_2-(CH_2)_6-NH_2$, $NH_2-(CH_2)_8-NH_2$ and $NH_2-(CH_2)_{10}-NH_2$ were denoted as $SiO_2/Pt/CNT(C6)$, $SiO_2/Pt/CNT(C8)$ and $SiO_2/Pt/CNT(C10)$, respectively.

2.2 Evaluation of electrocatalytic performance

Cyclic voltammetry (CV) data and polarization curves during the ORR on these Pt catalysts were acquired using a conventional three-electrode electrochemical system. A rotating-disk electrode method was applied to obtain the polarization curves for the ORR. Pt wire and a reversible hydrogen electrode (RHE) were used as the counter and reference electrode, respectively. The working electrode was prepared by first ultrasonically dispersing a Pt catalyst in 2-propanol to make a catalyst ink. An aliquot of the catalyst ink was dropped onto a glassy carbon electrode following which a Nafion solution diluted with methanol was dropped onto the electrode. The Pt loading on the working electrode was adjusted to be the same for each of the Pt catalysts (10 μg cm^{-2}). The working electrode thus obtained was immersed in a N_2-purged 0.1 M $HClO_4$ electrolyte at room temperature. The potential of the working electrode was repeatedly changed between 0.05 and 1.20 V (vs. RHE) for 50 cycles so as to clean the Pt metal surfaces. The CV data for the fresh Pt catalysts were acquired in a N_2-purged $HClO_4$

8

electrolyte at room temperature. Polarization curves for the ORR using fresh Pt catalysts were obtained in O_2-saturated 0.1 M $HClO_4$ at room temperature by changing the potential of the working electrode from 0.05 to 1.20 V. To assess the durability of the Pt catalysts, the potential of the working electrode was repeatedly changed between 0.05 and 1.20 V at 100 mV sec^{-1} with a triangular waveform in N_2-purged $HClO_4$ at room temperature. After the potential cycling, CV data and polarization curves for the ORR on the Pt catalysts were again acquired. The electrochemically active surface area (ECSA) of each Pt catalyst was determined from a voltammogram acquired during desorption of underpotentially deposited hydrogen, applying a value of 210 μC cm^{-2}-Pt during calculations.

2.3 Characterization of catalysts

The pore structures of the SiO_2/Pt/CNT catalysts were examined by adsorption and desorption of N_2 at the boiling temperature of liquid N_2, and the size distributions of the micropores and mesopores in these materials were calculated by applying the Holvath-Kawazoe and Barrett-Joyner-Halenda (BJH) models, respectively. The hydrophilic/hydrophobic properties of the SiO_2/Pt/CNT materials were evaluated by examining the adsorption of water molecules at 298 K. These assessments involving the

adsorption of N_2 and water molecules were performed with a Belsorp Max instrument (Bell, Japan). Prior to the adsorption trials, the catalysts were evacuated at 423 K for 12 h. Transmission electron microscopy (TEM) images of the catalysts were acquired using a FEI-TECNAI F20 (200 kV). Prior to these observations, each Pt catalyst was dispersed in 2-propanol and this suspension was dropped onto a grid to allow TEM image measurements. The Pt metal particle size distributions were evaluated by examining 200 particles randomly selected from TEM images. Fourier transform infrared (FT-IR) spectra of the SiO_2/Pt/CNT were acquired with a JASCO FT/IR 4200 by first thoroughly mixing samples of the Pt catalysts with KBr and then pressing the mixtures to obtain thin pellets.

3. Results and discussion

3. 1 SiO_2/Pt/CNT structures

Figure 1 presents TEM images of the Pt/CNT and SiO_2/Pt/CNT catalysts, while the Pt and Si contents of these catalysts are listed in Table 1. The Si loading levels were quite similar among all the SiO_2/Pt/CNT catalysts. The TEM image of the Pt/CNT shows that many Pt metal particles were supported on the CNT surfaces and that the diameters of most Pt particles ranged from 1 to 3 nm. As described in detail below, the

average diameter of the Pt metal particles in the Pt/CNT was estimated to be 2.2 nm.

The Pt/CNT is seen to be covered with silica layers and Pt metal particles are also

observed on the CNTs in the TEM images of all the SiO_2/Pt/CNT catalysts. In addition,

it is evident that the Pt particles sizes in the SiO_2/Pt/CNT catalysts are close to the sizes

in the Pt/CNT material, indicating that the silica coating process did not increase the Pt

particle size. In all the SiO_2/Pt/CNT materials, the Pt particles are seen to be covered

with a layer of silica a few nanometers thick.

Table 1 Pt and SiO_2 loading amounts in Pt/CNT and SiO_2/Pt/CNT catalysts

Catalyst	Pt loading / wt%	Si loading / wt%
Pt/CNT	15	-
SiO_2/Pt/CNT(TEOS)	10	10
SiO_2/Pt/CNT(MTEOS)	10	9
SiO_2/Pt/CNT(C6)	10	10
SiO_2/Pt/CNT(C8)	10	10
SiO_2/Pt/CNT(C10)	10	10

11
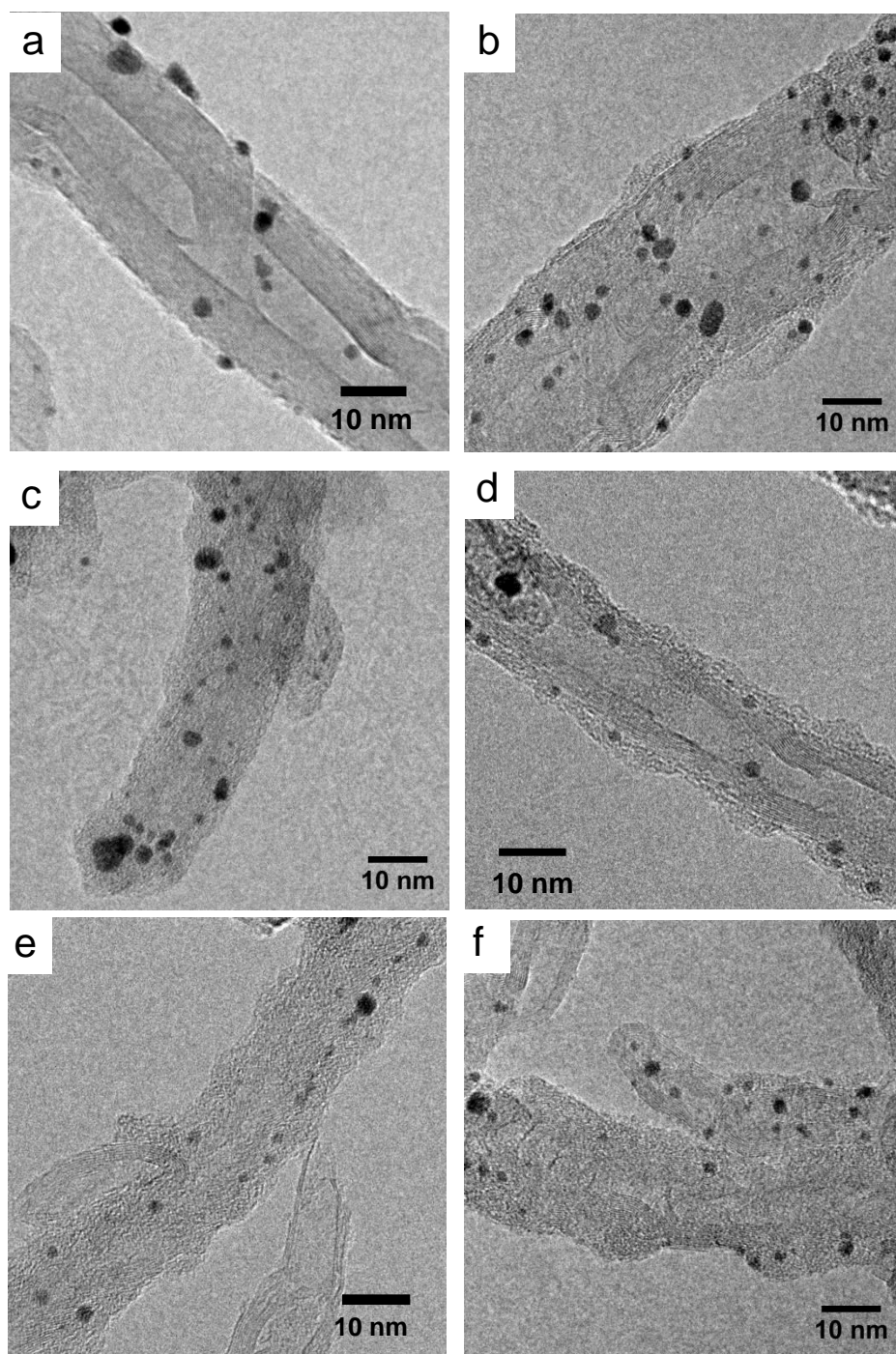
Fig. 1 TEM images of (a) Pt/CNT, (b) SiO$_2$/Pt/CNT(TEOS), (c) SiO$_2$/Pt/CNT(MTEOS), (d) SiO$_2$/Pt/CNT(C6), (e) SiO$_2$/Pt/CNT(C8) and (f) SiO$_2$/Pt/CNT(C10).

12
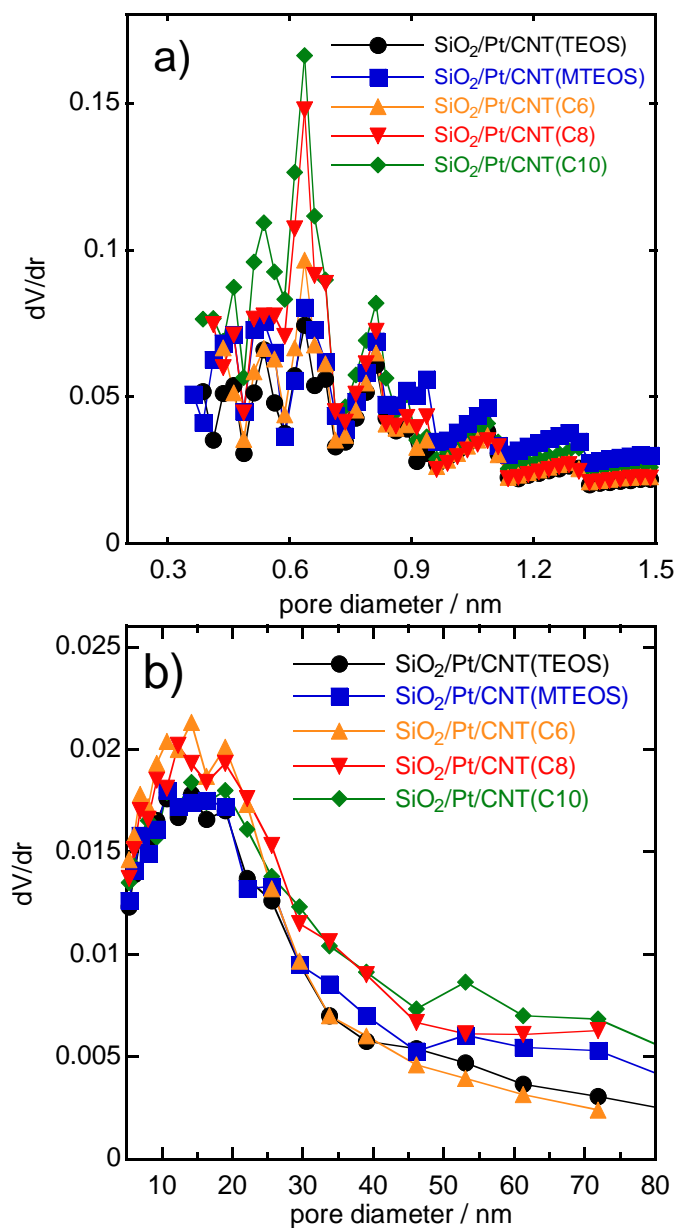
Fig. 2 Pore size distributions for Pt/CNT and SiO$_2$/Pt/CNT catalysts: (a) micropore range and (b) mesopore range.

Figure 2 shows the pore size distributions of the SiO$_2$/Pt/CNT catalysts in the micropore (panel a) and mesopore (panel b) ranges. The volumes of micropores and

13

mesopores for the SiO_2/Pt/CNT catalysts are summarized in Table 2. Only minimal pore

structure was found in the micropore range in the case of the SiO_2/Pt/CNT(TEOS) and

SiO_2/Pt/CNT(MTEOS). In contrast, the SiO_2/Pt/CNT catalysts prepared in the presence

of NH_2-$(CH_2)_n$-NH_2 had micropores of approximately 0.7 nm and the pore volume was

seen to gradually increase with n value of NH_2-$(CH_2)_n$-NH_2. These results suggest that

the NH_2-$(CH_2)_n$-NH_2 worked as molecular templates for the formation of micropores in

the silica layers. In contrast, there was little difference in the pore size distribution in the

mesopore range for all the SiO_2/Pt/CNT catalysts. The pore size distribution for all the

SiO_2/Pt/CNT catalysts had a maximum at around 15 nm. The volumes of both the

micropores and mesopores for the SiO_2/Pt/CNT catalysts prepared in the presence of

NH_2-$(CH_2)_n$-NH_2 were larger than those for the SiO_2/Pt/CNT(TEOS) and the volumes

became larger with the n value in NH_2-$(CH_2)_n$-NH_2. In the present study, the

silica-coated Pt catalysts were prepared by the successive hydrolysis of APTES and

TEOS in the presence of NH_2-$(CH_2)_n$-NH_2. APTES adsorbs on the Pt surfaces, primarily

through the interaction of N atoms in the APTES molecules with Pt surfaces, to form

very thin silica layers, after which the TEOS is hydrolyzed in the presence of

NH_2-$(CH_2)_n$-NH_2. Hydrolysis and polycondensation of the TEOS in a basic aqueous

solution (aqueous NH_3) forms silicate polyanions, and these should interact with the

14

positively charged NH_3^+ groups in NH_2-$(CH_2)_n$-NH_2 to form silica particles. The

resulting silica particles are deposited on the Pt/CNT surfaces to form silica layers. The

subsequent removal of the NH_2-$(CH_2)_n$-NH_2 by treatment of the SiO_2/Pt/CNT with

hydrogen at 623 K leads to the formation of micropores in the silica layers.

Table 2 Pore volumes of micropores and mesopores for SiO_2/Pt/CNT

Catalyst	Micropore volume / cm^3 g^{-1}	Mesopore volume / cm^3 g^{-1}
SiO_2/Pt/CNT(TEOS)	0.067	0.67
SiO_2/Pt/CNT(MTEOS)	0.089	0.80
SiO_2/Pt/CNT(C6)	0.074	0.68
SiO_2/Pt/CNT(C8)	0.086	0.83
SiO_2/Pt/CNT(C10)	0.098	0.94

Water molecules are formed during the ORR on the Pt catalysts, and these diffuse

out of the silica layers during the ORR on the SiO_2/Pt/CNT cathode catalysts. The ORR

activity of the SiO_2/Pt/CNT catalyst thus depends on the hydrophobic/hydrophilic

balance of the silica layers. To establish this balance, the amount of water adsorbed on

the SiO_2/Pt/CNT catalysts was evaluated, with the results shown in Fig. 3. Here the

amount of adsorbed water has been normalized by the specific surface area of each

catalyst, as determined by N_2 adsorption based on the Brunauer-Emmett-Teller (BET)

method. The resulting water adsorption isotherms were very similar among the

$SiO_2/Pt/CNT$ materials, with the exception of the $SiO_2/Pt/CNT$(MTEOS), which

adsorbed a significantly smaller quantity of water. This occurred because the methyl

groups in the silica layers rendered the surface of the $SiO_2/Pt/CNT$(MTEOS)

hydrophobic. The addition of NH_2-$(CH_2)_n$-NH_2 during the preparation of $SiO_2/Pt/CNT$

evidently did not change the hydrophobic/hydrophilic balance of the silica.
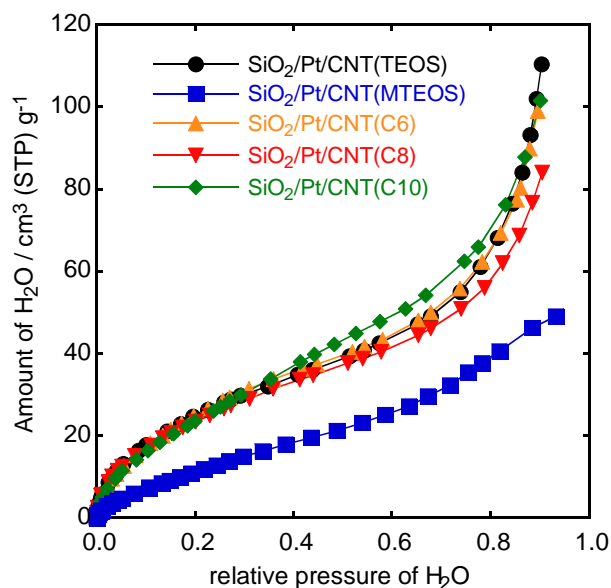
Fig. 3 Amount of water adsorbed on $SiO_2/Pt/CNT$ catalysts at 298 K as a
function of pressure.

16
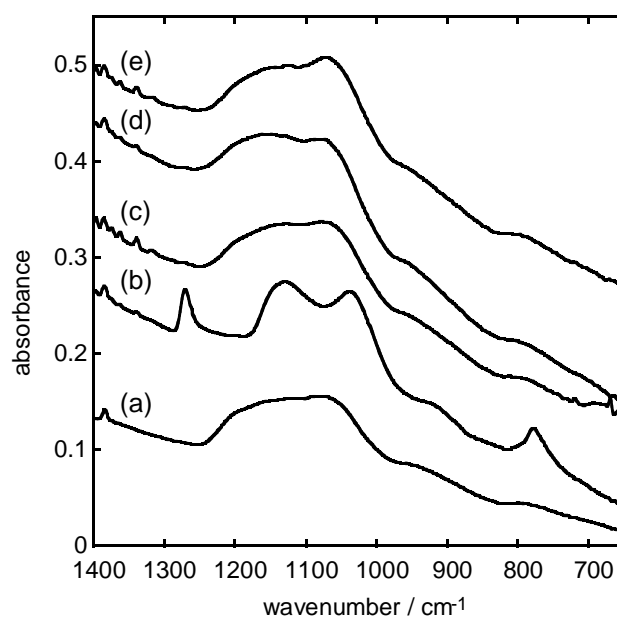
Fig. 4 FT-IR spectra of (a) SiO_2/Pt/CNT(TEOS), (b) SiO_2/Pt/CNT(MTEOS), (c) SiO_2/Pt/CNT(C6), (d) SiO_2/Pt/CNT(C8) and (e) SiO_2/Pt/CNT(C10).

Figure 4 shows the FT-IR spectra of the SiO_2/Pt/CNT catalysts. Two broad peaks were observed in the range from 1000 to 1200 cm^{-1} in the spectra of all the SiO_2/Pt/CNT, and these two peaks are assignable to the antisymmetric stretching of Si-O-Si (ν_{as} (Si-O-Si)) in siloxane rings.[21,22] In addition, the FT-IR spectra of all the SiO_2/Pt/CNT, except for SiO_2/Pt/CNT(MTEOS), exhibited two peaks at approximately 1080 and 1200 cm^{-1} due to the four-oxygen siloxane ring $(SiO)_4$ structure. In addition, no peaks due to $NH_2(CH_2)_nNH_2$ were observed in the SiO_2/Pt/CNT prepared in the presence of $NH_2(CH_2)_nNH_2$, indicating that the $NH_2(CH_2)_nNH_2$ molecules had been removed from

17

the silica layers. In contrast, there were two peaks at approximately 1030 and 1130 cm^{-1}

in the SiO$_2$/Pt/CNT(MTEOS) spectrum, attributed to the ν_{as} (Si-O-Si) vibration of the

six-oxygen siloxane ring (SiO)$_6$. Less intense peaks were also observed at 780 and 1140

cm^{-1} and these peaks can be assigned to the rocking mode of methyl groups bonded to

Si atoms and the stretching mode of Si-C, respectively, indicating the presence of

methyl groups in the silica layers of SiO$_2$/Pt/CNT(MTEOS).[23] As noted above, the silica

layers in all the SiO$_2$/Pt/CNT prepared from APTES and TEOS were composed of

four-oxygen siloxane rings, while (SiO)$_6$ was the main component of the silica layers of

the SiO$_2$/Pt/CNT prepared using APTES and MTEOS. These siloxane rings functioned

as conduits for the diffusion of oxygen and water molecules during the ORR on the

SiO$_2$/Pt/CNT, similar to catalytic reactions on zeolite catalysts. During this process, the

silica layers composed of (SiO)$_6$ would promote the diffusion of the reactants and

products to a greater extent since the associated pore sizes would be larger than those in

the (SiO)$_4$-based layers.

3.2 Catalytic performance of SiO$_2$/Pt/CNT

Figure 5 presents CV data obtained for the Pt/CNT and SiO$_2$/Pt/CNT catalysts

during the durability tests. Two peak couples are evident in the case of each Pt catalyst.

The peak couple in the potential range from 0.05 and 0.4 V is assignable to the adsorption and desorption of hydrogen on Pt metal while the other in the range from 0.5 and 1.2 V is due to the oxidation and reduction of Pt metal. The peak currents obtained for all the SiO_2/Pt/CNT catalysts were almost equal to that determined for the Pt/CNT, indicating that the majority of the Pt particles in the SiO_2/Pt/CNT catalysts were electrochemically active in spite of the silica coverage. The peak current exhibited by the Pt/CNT catalyst gradually decreased with prolonged potential cycling, due to the associated increases in the Pt particle size and the loss of Pt atoms from the working electrode due to the dissolution of Pt metal and the subsequent diffusion of dissolved Pt cations into the electrolyte. Compared to the decreases in the peak current observed with the Pt/CNT, the decrease associated with durability testing of the SiO_2/Pt/CNT(TEOS) was insignificant. In addition, the peak current obtained for the SiO_2/Pt/CNT(TEOS) was very high, even after 1500 cycles. The silica layers in the SiO_2/Pt/CNT(TEOS) evidently inhibited the outward diffusion of dissolved Pt cations as well as the migration of Pt particles over the CNT support. In contrast, the peak currents for the SiO_2/Pt/CNT materials other than the SiO_2/Pt/CNT(TEOS) were found to slightly decrease with extended potential cycling.

19
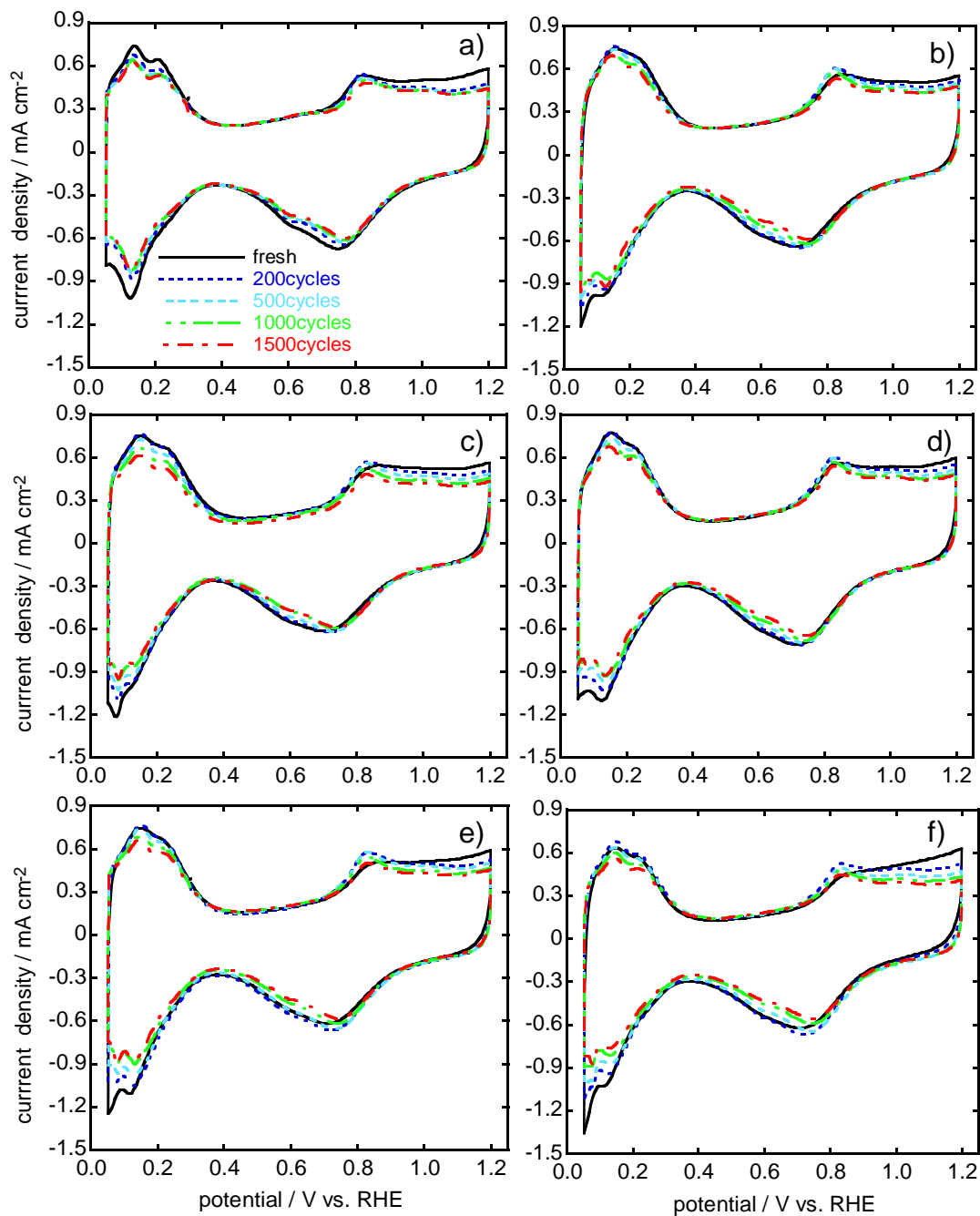
Fig. 5 CV data for (a) Pt/CNT, (b) SiO$_2$/Pt/CNT(TEOS), (c) SiO$_2$/Pt/CNT(MTEOS), (d) SiO$_2$/Pt/CNT(C6), (e) SiO$_2$/Pt/CNT(C8) and (f) SiO$_2$/Pt/CNT(C10) catalysts during durability testing. Scan rate = 50 mV s^{-1}.
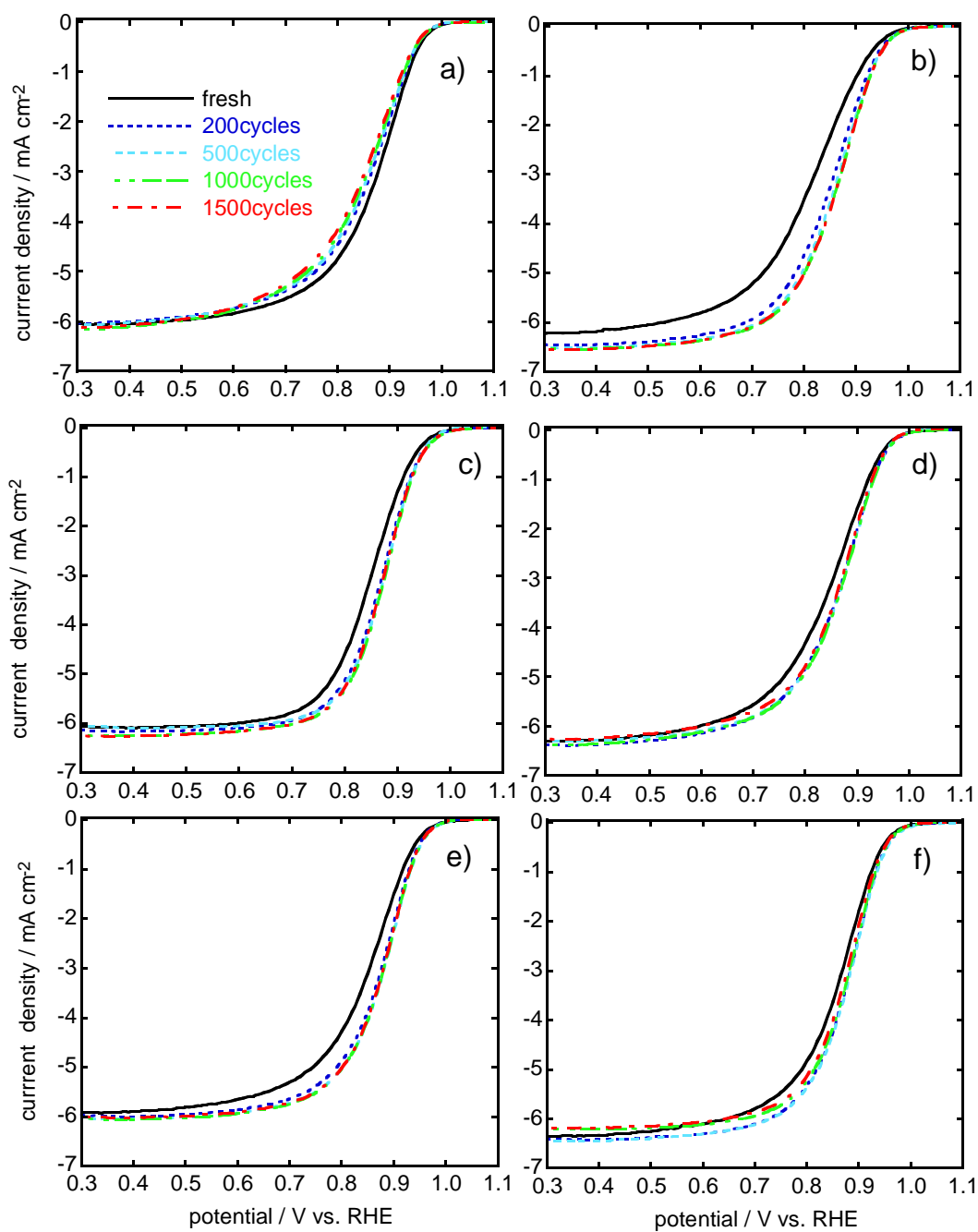
Fig. 6 Polarization curves associated with the ORR on (a) Pt/CNT, (b) SiO₂/Pt/CNT(TEOS), (c) SiO₂/Pt/CNT(MTEOS), (d) SiO₂/Pt/CNT(C6), (e) SiO₂/Pt/CNT(C8) and (f) SiO₂/Pt/CNT(C10) during durability testing. Scan rate = 10 mV s-1; rotation rate of the working electrode = 1600 rpm.

21

Figure 6 shows the polarization curves associated with the ORR on the Pt/CNT and

SiO$_2$/Pt/CNT catalysts during the durability tests. All the Pt catalysts exhibited catalytic

activity for the ORR. The ORR currents reached a diffusion-limited value at higher

overpotential values ($<$ 0.7 V), while the reaction exhibited mixed kinetic/diffusion

control at lower overpotentials ($>$ 0.8 V). The ORR currents of the Pt/CNT catalysts at

approximately 0.9 V gradually decreased as the number of potential cycles was

increased, due to the loss of Pt atoms from the catalysts and increases in the Pt particle

sizes during the durability test. Each of the fresh SiO$_2$/Pt/CNT catalysts showed a

slightly lower activity for the ORR than the fresh Pt/CNT catalyst. However, the ORR

activity of the SiO$_2$/Pt/CNT catalysts was marginally enhanced after 200 cycles of the

potential cycling test and then remained unchanged after further potential cycling. This

result indicates that coverage with silica layers prevented the deactivation of the Pt/CNT

catalysts with regard to the ORR. The increase in the catalytic activity of the

SiO$_2$/Pt/CNT catalysts at early period of the durability test would be due to the removal

of impurities on the Pt metal surfaces which had been deposited during the

silica-coating process. Additionally, the increase in the catalytic activity for the ORR

was also observed during the durability test for the silica-coated Pd/CNT catalysts.[24]

The increase in the catalytic activity of the Pd catalysts was assignable to the change of

22

morphology of Pd metal particles, which resulted from the dissolution of Pd cations from Pd metal and the subsequent deposition of the cations on the Pd metal. It is likely that the catalytically active Pt metal facets for the ORR are formed during the durability test of the SiO_2/Pt/CNT catalysts.
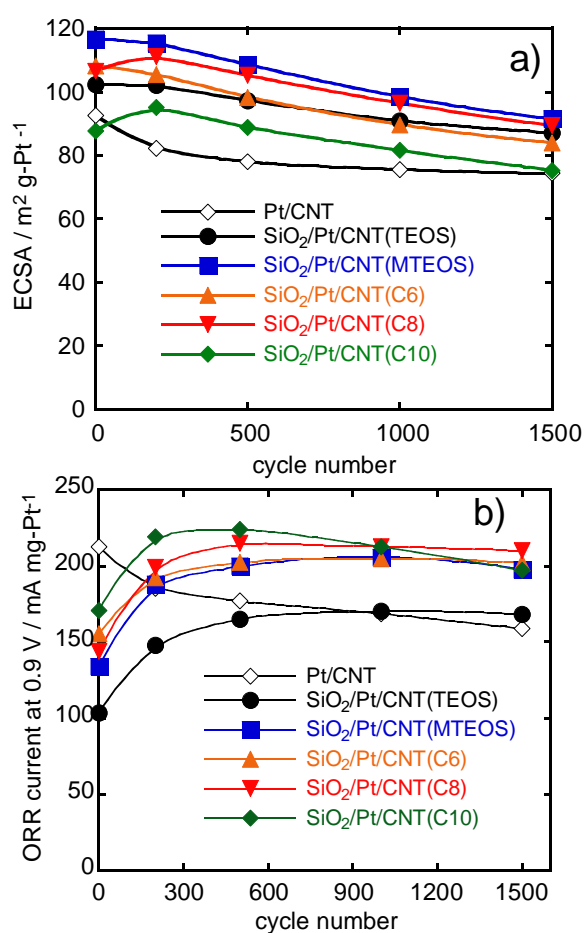
Fig. 7 Variations in the (a) ECSA and (b) ORR current at 0.9 V for Pt/CNT and SiO_2/Pt/CNT catalysts during durability testing.

The changes in the ECSA and ORR current at 0.9 V during the durability tests for all the Pt catalysts are summarized in Fig. 7. The ECSA for the Pt/CNT was significantly decreased during the potential cycling up to the 500 cycles mark, after which it was gradually reduced by further potential cycling. The ESCA values for the SiO_2/Pt/CNT materials also decreased during the durability test, but this decrease was mitigated by silica layers, such that the ECSA values obtained for the SiO_2/Pt/CNT catalysts were always higher than that of the Pt/CNT.

The ORR current at 0.9 V measured for the Pt/CNT material also decreased rapidly during the initial stages of the durability tests, such that the ORR current from the Pt/CNT dropped from 220 to 150 mA mg-Pt^{-1} after 1500 cycles. In contrast, the ORR currents from each of the SiO_2/Pt/CNT catalysts were slightly increased and these elevated values were maintained over the durability test. The ORR activity of the SiO_2/Pt/CNT(TEOS) was especially stable and did not decrease at all during the test, although this material exhibited the lowest activity for the ORR among all the SiO_2/Pt/CNT catalysts tested in the present study. The hydrophilic silica layers prepared from APTES and TEOS were composed of the four membered siloxane ring and the smaller porous structures in this silica evidently inhibited the diffusion of the reactants and products to or from the Pt surfaces, while the hydrophilic silica made the diffusion

24

of products more difficult. The utilization of MTEOS as a silica source in the $SiO_2/Pt/CNT$ catalyst enhanced its ORR activity during the durability tests. As described earlier, the hydrophobic silica prepared from MTEOS was composed of six membered siloxane rings, and the larger pores and hydrophobic nature of this silica promoted the diffusion of reactants and products during the ORR. It is interesting to observe that the $SiO_2/Pt/CNT$ catalysts prepared from APTES and TEOS in the presence of $NH_2(CH_2)_nNH_2$ also showed increased ORR activity compared to the $SiO_2/Pt/CNT$ prepared from APTES and TEOS in the absence of $NH_2(CH_2)_nNH_2$. The ORR activity of the $SiO_2/Pt/CNT$ prepared with $NH_2(CH_2)_nNH_2$ was also found to increase with higher values of n. The pore structures formed by the $NH_2(CH_2)_nNH_2$ templates thus appear to have functioned as diffusion paths for both the reactants and products during the ORR.

Figure 8 shows representative TEM images of the Pt catalysts after the durability tests. The distributions of Pt particle sizes before and after these tests were determined from these images, with the results summarized in Fig. 9. This figure also presents the average particle sizes for each catalyst before and after the durability trials. Many Pt particles were observed in the TEM images of the used Pt/CNT and $SiO_2/Pt/CNT$ catalysts. Interestingly, particles smaller than 2 nm in diameter were frequently seen in

25

the TEM images of all the SiO_2/Pt/CNT catalysts following the durability tests, whereas

they were seldom present in the TEM images of used Pt/CNT. Following cycling, the Pt

particle size distribution of the Pt/CNT was shifted towards larger sizes, while the

average particle size increased from 2.2 to 4.0 nm. The size distributions of all the

SiO_2/Pt/CNT catalysts were also shifted towards larger sizes, but the increment in the

average particle size was significantly smaller than that for the Pt/CNT catalysts. Thus,

the silica layers around the Pt particles evidently inhibited both the aggregation of these

particles and the diffusion of Pt cations and their subsequent redeposition on other Pt

metal particles, regardless of the type of silica layer. The successive hydrolysis of

APTES and TEOS in the presence of the $NH_2(CH_2)_nNH_2$ templates is thus an effective

means of preparing silica-coated Pt catalysts with high ORR activity and excellent

durability. The pore structures formed from these $NH_2(CH_2)_nNH_2$ templates create gaps

among the silica particles and these gaps together with the siloxane rings in the silica

layers act as diffusion paths for reactants and products. Additionally, the silica layers

prevent the outward diffusion of dissolved Pt cations.
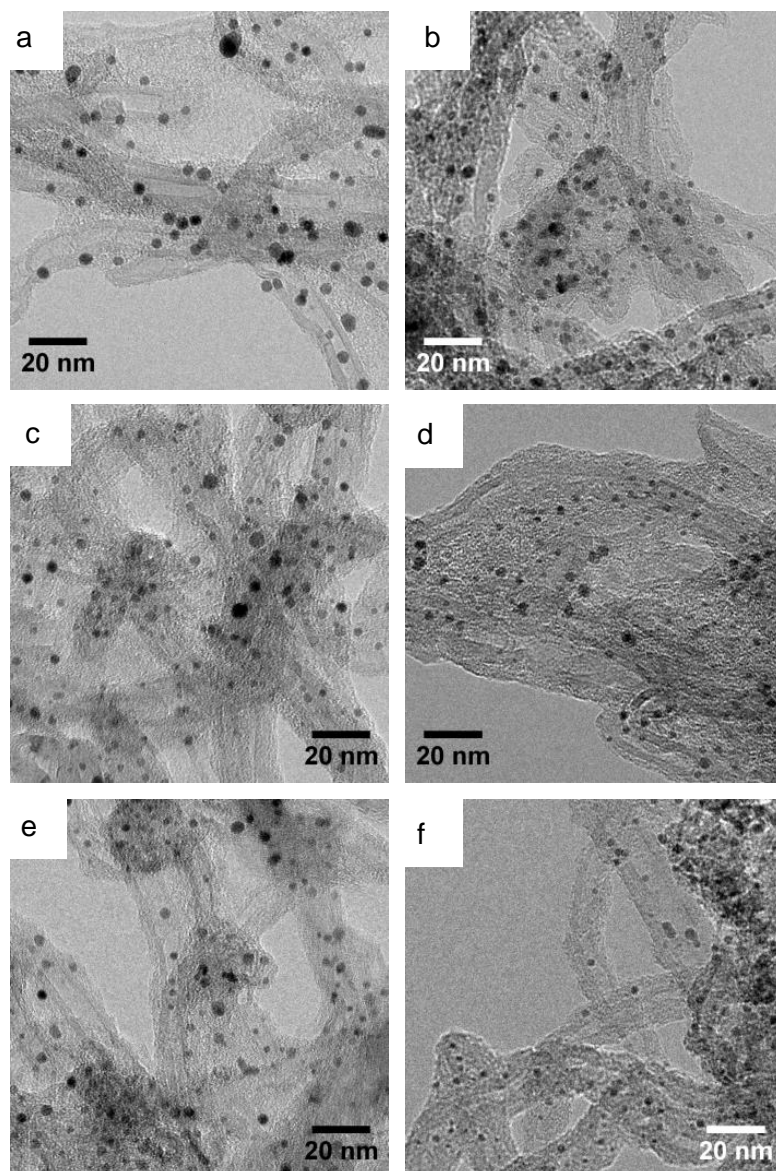
Fig. 8 TEM images of (a) Pt/CNT, (b) SiO$_2$/Pt/CNT(TEOS), (c) SiO$_2$/Pt/CNT(MTEOS), (d) SiO$_2$/Pt/CNT(C6), (e) SiO$_2$/Pt/CNT(C8) and (f) SiO$_2$/Pt/CNT(C10) following durability testing.

27
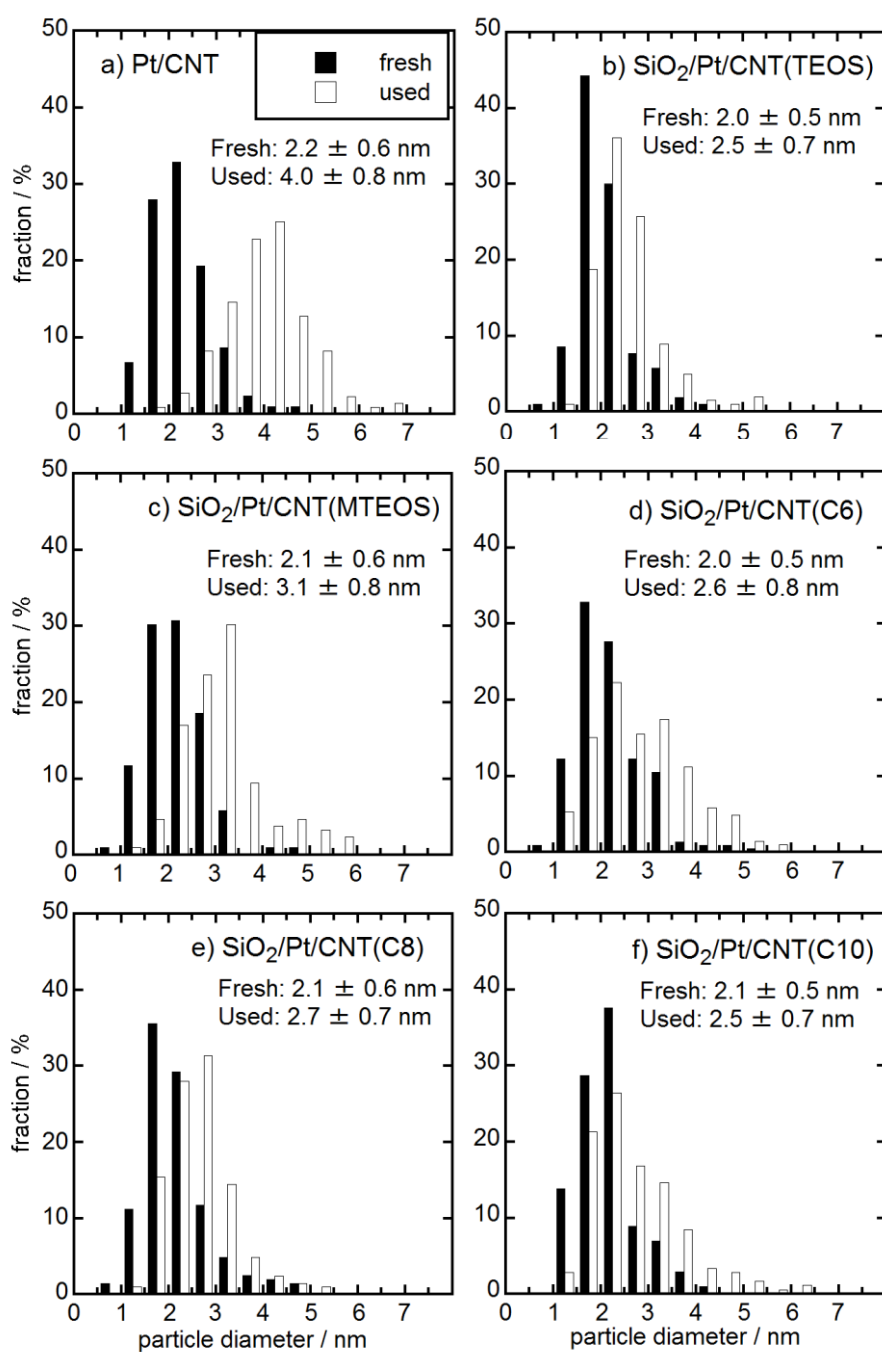
Fig. 9 Pt particle size distributions in catalysts before and after durability testing.

4. Conclusion

SiO$_2$/Pt/CNT catalysts were prepared by the successive hydrolysis of APTES and TEOS in the presence of NH$_2$(CH$_2$)$_n$NH$_2$ molecules that functioned as templates for the formation of micropores in the silica layers. The resulting pore structures acted as diffusion paths for both reactants and products. As a result, the SiO$_2$/Pt/CNT catalysts exhibited high ORR activity and excellent durability under PEFC cathode conditions.

Notes and references

1   G. A. Gruver, R. F. Pascoe and H. R. Kunz, *J. Electrochem. Soc.*, 1980, **127**, 1219-1224.

2   A. C. C. Tseung and S. C. Dhara, *Electrochim. Acta*, 1975, **20**, 681-683.

3   A. Honji, T. Mori, K. Tamura and Y. Hishimura, *J. Electrochem. Soc.*, 1988, **135**, 355-359.

4   E. Guilminot, A. Corcella, F. Charlot, F. Maillard and M. Chatenet, *J. Electrochem. Soc.*, 2007, **154**, B96-B105.

5   X. Li, X. Wang, D. Liu, S. Song and H. Zhang, *Chem. Commun.*, 2014, **50**, 7198-7201.

6   T. Zhang, H. Zhao, S. He, K. Liu, H. Liu, Y. Yin and C. Gao, *ACS Nano*, 2014, **8**,

7297-7304.

7   K. An, Q. Zhang, S. Alayoglu, N. Musselwhite, J. Shin and G. A. Somorjai, *Nano Lett.*, 2014, **14**, 4907-4912.

8   P. Lu, C. T. Campbell and Y. Xia, *Nano Lett.*, 2013, **13**, 4957-4962.

9   S. Takenaka, Y. Orita, H. Matsune, E. Tanabe and M. Kishida, *J. Phys. Chem. C*, 2007, **111**, 7748-7756.

10   S. Takenaka, T. Arike, K. Nakagawa, H. Matsune and M. Kishida, *Carbon*, 2008, **46**, 365-368.

11   S. Takenaka, T. Arike, H. Matsune, E. Tanabe and M. Kishida, *J. Catal.*, 2008, **257**, 345-355.

12   S. Takenaka, H. Matsumori, K. Nakagawa, H. Matsune, E. Tanabe and M. Kishida, *J. Phys. Chem. C*, 2007, **111**, 15133-15136.

13   S. Takenaka, H. Matsumori, H. Matsune and M. Kishida, *Appl. Catal. A: Gen.*, 2011, **409-410**, 248-256.

14   S. Takenaka, H. Miyamoto, Y. Utsunomiya, H. Matsune and M. Kishida, *J. Phys. Chem. C*, 2014, **118**, 774-783.

15   J. Yang, F. Zhang, W. Li, D. Gu, D. Shen, J. Fan, W. Zhang and D. Zhao, *Chem. Commun.*, 2014, **50**, 713-715.

16 L. Shang, T. Bian, B. Zhang, D. Zhang, L. Wu, C. Tung, Y. Yin and T. Zhang, *Angew. Chem. Int. Ed.*, 2014, **53**, 250-254.

17 X. Wang, W. Li, Z. Chen, M. Waje and Y. Yan, *J. Power Sources*, 2006, **158**, 154-159.

18 Y. Shao, G. Yin, Y. Gao and P. Shi, *J. Electrochem. Soc.*, 2006, **153**, A1093-A1097.

19 S. Takenaka, N. Susuki, H. Miyamoto, E. Tanabe, H. Matsune and M. Kishida, *Chem. Commun.*, 2010, **46**, 8950-8952.

20 S. Takenaka, T. Tsukamoto, H. Matsune and M. Kishida, *Catal. Sci. Technol.*, 2013, **3**, 2723-2731.

21 A. Fidalgo and L. M. Ilharco, *Chem. Eur. J.*, 2004, **10**, 392-398.

22 A. Figalgo, R. Ciriminna, L. M. Ilharco and M. Pagliaro, *Chem. Mater.*, 2005, **17**, 6686-6694.

23 M. N. Ghazzal, M. Joseph, H. Kebaili, J. De Coninck and E. M. Gaigneaux, *J. Mater. Chem.*, 2012, **22**, 22526-22532.

24 S. Takenaka, N. Susuki, H. Miyamoto, E. Tanabe, H. Matsune and M. Kishida, *J. Catal.*, 2011, **279**, 381-388.